Article

The potential role of non-coding RNAs RP11-573G6.6 and HCG11 in the regulation of mitochondrial gene expression in glioblastoma: A bioinformatics-based study

Mahya Payazdan[1], **Mohammad Shafiei**[1], **Seyedeh Sahar Mortazavi Farsani**[2]
[1]Department of Biology, Faculty of Science, Shahid Chamran University of Ahvaz, Ahvaz, Iran
[2]Department of Genetics, Faculty of Biological Science, Tarbiat Modares University, Tehran, Iran
Email: Mahyapayazdan@yahoo.com

Received 7 April 2021; Accepted 15 May 2021; Published 1 September 2021

Abstract
Long non-coding RNAs (lncRNAs) have attracted lots of attention worldwide. With the rapid advances in bioinformatics, several lncRNAs have been identified in the last decade. Ample evidence has shown that lncRNAs are involved in different mechanisms and play chief roles in many biological processes. Therefore, dysregulations of lncRNAs are associated with human complex diseases including glioblastoma (GBM). In this study, we have used lncRNA high throughput data analysis and some databases about their expression level, function, etc. Currently, a limited number of GBM-related lncRNAs have been reported experimentally. Therefore, analyzing lncRNA-GBM associations and predicting potential lncRNAs would benefit mechanism understanding, diagnosis, treatment, and prevention of this tumor. Therefore, we applied *in silico* analysis to find GBM-related lncRNAs and select the most promising lncRNAs for experimental validation. According to the results RP11-573G6.6 and HCG11, lncRNAs play critical role in GBM pathogenesis and could be promising targets in novel therapeutic approaches.

Keywords Glioblastoma; *in silico*; lncRNAs; mitochondrial gene expression; RNA sequencing.

Network Biology
ISSN 2220-8879
URL: http://www.iaees.org/publications/journals/nb/online-version.asp
RSS: http://www.iaees.org/publications/journals/nb/rss.xml
E-mail: networkbiology@iaees.org
Editor-in-Chief: WenJun Zhang
Publisher: International Academy of Ecology and Environmental Sciences

1 Introduction

Glioblastoma, also known as glioblastomamultiforme (GBM), is the most common and the most aggressive type of primary malignant brain tumor associated with high morbidity and mortality (Louis et al., 2016; Van Meir et al., 2010). Despite advances in new techniques of radiotherapy and chemotherapy and also multimodality treatment efforts, the median survival for GBM remains less than 14 months (Bai et al., 2011). Due to this high mortality, attention has been given to understand the GBM pathogenesis (Alifieris and Trafalis 2015). This tumor is highly variable at the molecular level and shows momentous heterogeneity in each tumor. Molecular analysis of these tumors and finding diagnostic and therapeutic options therefore have

fundamental implications for targeted therapeutic strategies (Parker et al., 2015). Recently, there is growing evidence demonstrating that the discovery and use of molecular markers facilitate the identification and also the treatment of this tumor (Ducray et al., 2009). More recently, dysregulated functional non-coding RNAs (ncRNAs) as molecular markers in human diseases have attracted extensive attention. Actually, only 2% of the genome is involved in protein-encoding, and at least 75% of the total is transcribed into ncRNAs that do not encode for a protein including lncRNAs and small ncRNAs (Ponting et al., 2009). LncRNAs are defined as a heterogeneous class of ncRNAs with a length of more than 200 nucleotides. They have been shown to get involved in transcriptional and post-transcriptional regulation (Yoon et al., 2012). Furthermore, existing research displays that lncRNAs are associated with various biological processes such as cellular development and differentiation, proliferation, DNA damage response, and many others (Sánchez and Huarte, 2013; Fang and Fullwood, 2016). Increasing evidence has shown that lncRNAs are involved in the regulation of various biological processes in carcinomas, including GBM, and are therefore known as new modulators in the development of GBM (Huarte, 2015; Qureshi and Mehler, 2012). However, little is known about the role of functional lncRNAs in this tumor and only a few of them have been well characterized. Recent advances in computational methods have led to identifying noteworthy lncRNAs and also a better understanding of the key molecular changes that underlie GBM which results in better treatment design (Zhou et al., 2018). Using an lncRNA-mining approach, in this study we performed an *in silico* study to identified differently expressed lncRNAs in GBM. The role of RP11-573G6.6 and HCG11 in the regulation of mitochondrial gene expression in GBM was elucidated. Then, the Kyoto Encyclopedia of Genes and Genomes (KEGG) pathway and Gene Ontology (GO) analysis, as well as network analysis were used to assess the potential functions of lncRNAs. Overall, this study could provide novel biomarkers for the diagnosis and treatment of GBM.

2 Materials and Methods

2.1 RNA-seq data analysis

Transcriptome data can be seen in Table 1 was analyzed using the Galaxy web interface as a web-based analysis platform (https://galaxyproject.org) (Afgan et al., 2018) and read quality was assessed via FastQC (Galaxy Version 20.09)(Andrews, 2010). Then, HiSAT2 software (Galaxy Version 20.09) was applied to align the RNA-seq reads to the human genome and Homo Sapiens (hg38) was utilized as a reference genome (Kim et al., 2019). Subsequently, we used StringTie software (Galaxy Version 20.09) as a highly effective assembler of RNA-Seq alignments to count aligned reads (Pertea et al., 2015). The DESeq2 method (Galaxy Version 20.09) was used for differential gene expression analysis and only genes with p-value ≤ 0.05 were considered differentially expressed (Love et al., 2014).

Table 1 RNAseq data.

Experiment	Glioblastoma	Control	Platform	Sample
GSE86202	3	3	IlluminaHiSeq 2500	Brain tissue
GSE151352	12	12	Ion Torrent S5	Brain tissue

2.2 GO function and KEGG pathway enrichment analysis

R Language Cluster Profiler package were applied to analyze both Gene ontology (GO) functional classification and enrichment analysis (p-value Cutoff = 0.05, q-value Cutoff = 0.05) and KEGG pathway (p-value Cutoff = 0.05, q-value Cutoff = 0.05) (Love et al., 2014).

2.3 Construction and analysis of PPI network complex

STRING (The Retrieval of Interacting Genes Database) (https://string-db.org/) is a biological database providing protein-protein interactions (PPI) information. This database includes information from experimental data, and computational prediction methods (Szklarczyk et al., 2015). The STRING database was used to explore the interactions between the common differentially expressed genes (DEGs) which were obtained, and we also used Cytoscape software to visualize the results. MCODE, a Cytoscape plug-in, provided access to select hub modules of PPI in a network (Shannon et al., 2003). The criteria default parameters as follows: k-core = 2, degree cut-off = 2, max. Depth = 100 and node score cut-off = 0.2. To recognize genes in the hub module, a cluster profiler was used again for functional enrichment analysis, and subsequently, the hub genes were extracted using CytoHubba. Through the CytoHubba plugin, 12 topological analysis methods were found (Chin et al., 2014). The top 3 hub-forming genes/proteins were found.

2.4 LncRNA/mRNA interaction

Co-expression relationships between the lncRNAs and the protein-coding genes were assessed by Pearson's correlation test in R (version 3.6.2) software. Differently expressed lncRNAs and their significantly correlated mRNAs were considered to draw the network with Cytoscape (version 3.7.2).

3 Results

A total of 4851 and 210 genes with a P-value less than 0.05 were found in the GSE86202 dataset and GSE151352 dataset respectively (Fig. 1).

A total of 109 overlapped genes were extracted using the Venn Diagram (http://bioinformatics.psb.ugent.be/webtools/Venn/) (Fig. 2).

The expression and P-value of overlapped genes in the selected studies are represented in Table 2. The expression of these 109 genes in each sample of the two studies was also shown in a heatmap (Fig. 3).

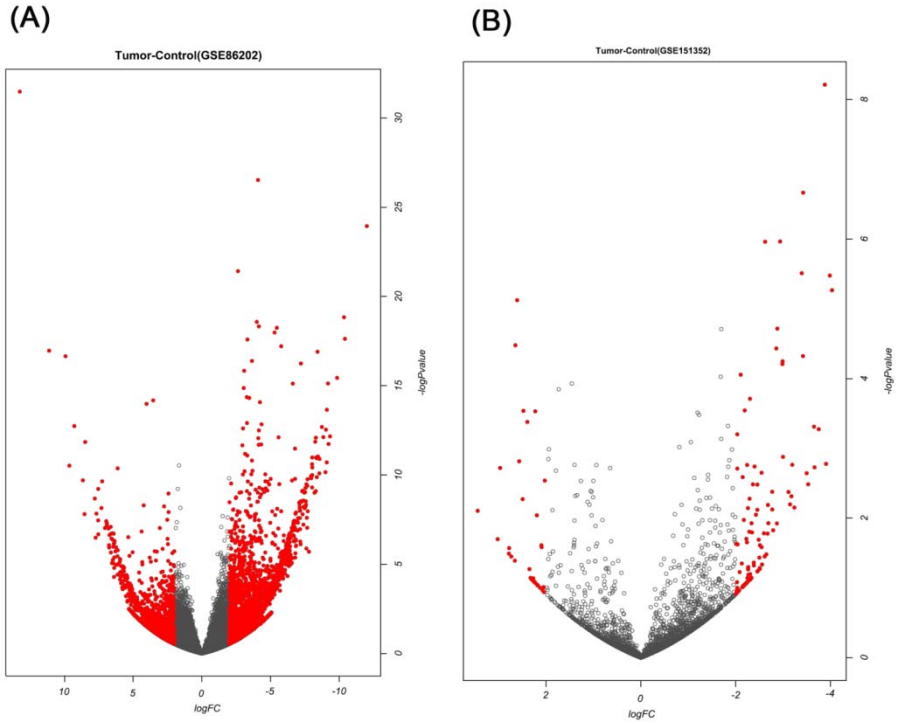

Fig. 1 Volcano Plot related to A) Total genes with p-value less than 0.05 in GSE86202 dataset and B) Total genes with p-value less than 0.05 in GSE151352 dataset.

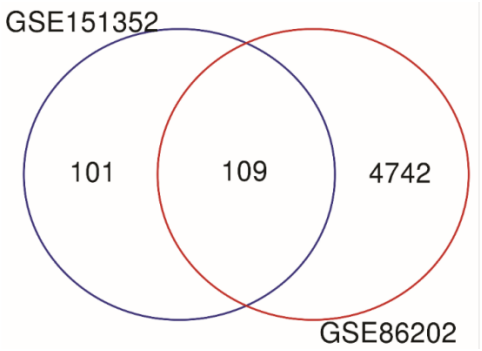

Fig. 2 A total of 109 overlapped genes between two studies.

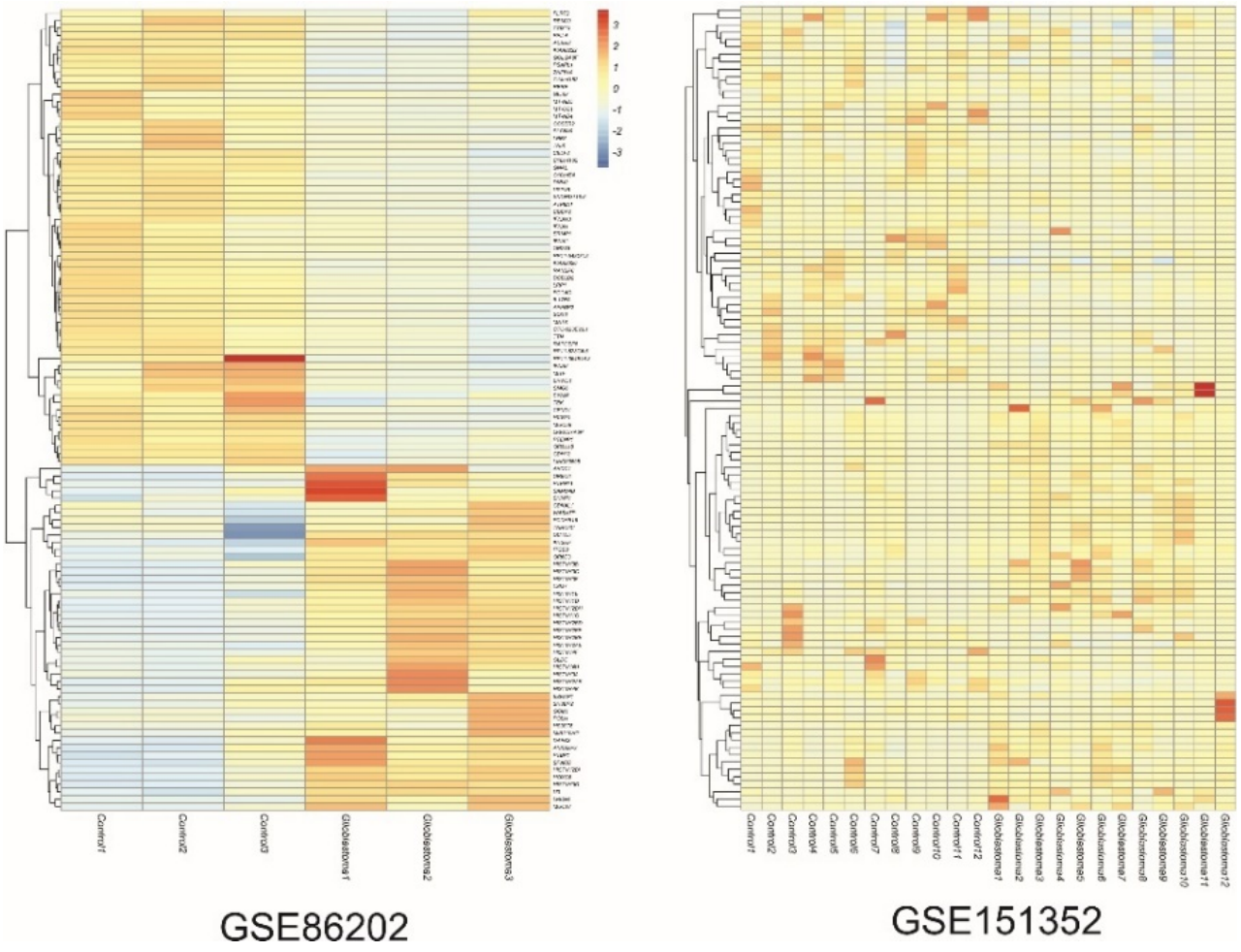

Fig. 3 The heat map corresponds to the expression level of 109 common genes in each sample.

Table 2 Expression level and P-value of common genes in two studies.

Gene symbol	Ensembl ID	GSE86202		GSE151352	
		log2 (FC)	P-value	log2(FC)	P-value
ACER2	ENST00000340967	-0.92439	0.008446	-2.93603	1.08E-06
AHDC1	ENST00000646642	2.329249	0.033568	-1.82233	0.051625
ANXA2P2	ENST00000426153	2.31776	0.024915	1.949792	0.001424
APPBP2	ENST00000083182	-3.59057	3.38E-10	-2.38027	0.043415
ATP8A1	ENST00000381668	-4.11575	8.69E-13	-2.23614	0.022211
BRWD1	ENST00000342449	-4.15748	4.76E-19	-2.12716	0.044661
BZRAP1	ENST00000355701	1.801038	0.010656	-1.40895	0.024284
C10orf105	ENST00000441508	-2.46155	5.65E-08	-2.009	0.023451
C10orf54	ENST00000394957	-1.32171	0.002002	-2.29119	0.005264
C14orf182	ENST00000399206	-1.24508	0.027207	-2.76875	0.007508
CCSER2	ENST00000224756	-2.13239	0.000504	-2.4546	0.007593
CDCA2	ENST00000330560	-3.60615	9.15E-11	-1.61281	0.024817
CDH13	ENST00000566620	-0.966	0.039536	-1.66339	0.016059
CDKAL1	ENST00000274695	0.745617	0.036995	-1.26984	0.057022
CELF2	ENST00000379261	-1.36465	0.043937	-1.21724	0.044355
CEND1	ENST00000330106	-1.5742	0.000117	-1.93396	0.008947
COX14	ENST00000550487	-1.39102	0.007905	-1.45636	0.010692
CTC-523E23.1	ENST00000561778	-4.43124	0.000691	-3.1443	0.00635
DAPK3	ENST00000545797	1.343237	0.031748	0.94757	0.025381
DCBLD2	ENST00000326840	-2.99668	7.61E-08	-2.2612	0.054243
DCTN5	ENST00000300087	1.187836	0.002034	1.748943	0.049762
DNM3	ENST00000358155	-2.83418	0.000288	-2.99611	0.001322
ERMP1	ENST00000339450	-5.19543	0.000226	-1.92047	0.001039
FOCAD	ENST00000380249	-1.39964	0.001009	-1.69309	0.000732
GCM1	ENST00000259803	0.795224	0.045104	1.22849	0.052886
GLDC	ENST00000321612	1.203492	0.053106	3.020103	0.02001
GNAL	ENST00000334049	-2.41052	7.21E-08	-2.86754	0.011923
GOLGA8F	ENST00000526619	-0.95829	0.001641	-1.41682	0.002393
HCG11	ENST00000411553	-2.01944	1.50E-07	-2.34298	0.016015
HIST1H1C	ENST00000343677	1.583037	0.000683	1.398955	0.001719
HIST1H1D	ENST00000244534	2.858958	0.000241	1.732041	0.000142
HIST1H1E	ENST00000304218	1.595	0.000265	0.956392	0.012931
HIST1H2AB	ENST00000259791	2.713195	0.024399	2.025183	0.002894
HIST1H2AE	ENST00000303910	1.69979	5.70E-05	1.040369	0.009124
HIST1H2BD	ENST00000377777	3.059881	9.38E-08	1.106006	0.042063
HIST1H2BE	ENST00000356530	2.255335	2.22E-05	1.456406	0.000118
HIST1H2BF	ENST00000359985	2.275923	9.68E-06	1.345888	0.004676
HIST1H2BH	ENST00000356350	3.330695	0.000769	1.939894	0.001028
HIST1H2BI	ENST00000377733	3.32683	6.55E-05	2.608898	7.51E-06
HIST1H3A	ENST00000357647	1.834295	0.010046	1.123063	0.005839

Gene symbol	Ensembl ID	GSE86202		GSE151352	
		log2 (FC)	P-value	log2(FC)	P-value
HIST1H3B	ENST00000244661	2.96976	0.011347	1.793676	0.002083
HIST1H3C	ENST00000540144	4.332482	1.03E-05	2.2274	0.000294
HIST1H3F	ENST00000446824	3.639764	0.00148	2.646263	3.32E-05
HIST1H3G	ENST00000305910	3.551631	0.001931	2.394536	0.000418
HIST1H4B	ENST00000377364	1.576506	0.035705	1.058994	0.004073
HIST1H4F	ENST00000377745	2.505499	0.000159	2.092219	0.025997
HIST1H4H	ENST00000377727	1.411921	0.017862	1.084119	0.006424
HOXC8	ENST00000040584	1.791915	0.003366	1.417364	0.026152
HS3ST6	ENST00000443547	1.184542	0.036486	0.962369	0.041368
IFNA1	ENST00000276927	-3.01617	0.031691	-2.85547	3.69E-05
IFNA13	ENST00000449498	-3.65737	0.046477	-3.39071	3.08E-06
IFNA2	ENST00000380206	-5.67428	0.000151	-3.41811	4.75E-05
IFNA8	ENST00000380205	-3.75256	0.015381	-2.50979	0.024463
IL17RA	ENST00000319363	-1.42996	0.000334	-1.82596	0.012315
ITGB8	ENST00000222573	3.561464	0.007786	2.968351	0.001909
KHSRP	ENST00000398148	1.235108	0.008779	0.685364	0.052267
KIAA0232	ENST00000307659	-0.95766	0.004258	-2.68765	0.011804
KIAA2026	ENST00000399933	-1.01599	0.01139	2.657938	0.040735
LINC00598	ENST00000400430	-1.03835	0.008825	-1.98548	0.038955
LRBA	ENST00000510413	-1.60087	0.016237	-2.03184	0.000628
LRCH4	ENST00000310300	2.517906	3.24E-08	2.566669	0.001532
LRP1	ENST00000243077	-2.87881	6.05E-07	-3.52727	0.003264
LRRC37A6P	ENST00000448648	-1.57738	0.004212	-1.19878	0.003962
LSM7	ENST00000252622	1.70144	0.001312	1.007773	0.005019
MATK	ENST00000310132	-2.5564	0.00735	-3.9044	0.001666
MIR210HG	ENST00000500447	2.471826	0.001893	1.863773	0.007699
MITF	ENST00000352241	-3.48317	0.003374	-2.50621	0.051999
MT-CO1	ENST00000361624	-2.01998	0.004584	-1.68413	9.37E-05
MT-ND4	ENST00000361381	-1.62436	0.008119	-1.38229	0.005128
MT-ND5	ENST00000361567	-1.27629	0.013104	-1.41304	0.0028
MUC17	ENST00000306151	1.767869	0.002968	1.001419	0.002931
MUC5B	ENST00000447027	-0.81995	0.059909	-2.33313	0.011835
OR2T8	ENST00000319968	-3.91338	0.016412	-3.98342	3.33E-06
OR5H15	ENST00000356526	-1.24872	0.001252	-1.88243	0.051818
OR6C3	ENST00000379667	1.897442	9.39E-08	0.925041	0.023102
OR6C6	ENST00000358433	2.656523	0.00166	0.964638	0.041351
PCDHB16	ENST00000361016	0.649723	0.030141	-2.18918	0.000285
PSAPL1	ENST00000319098	-1.59782	0.007921	-1.97582	0.018494
PTBP1	ENST00000356948	1.779227	0.01009	1.265473	0.002932
PTENP1	ENST00000532280	-1.19383	0.028207	-1.1246	0.002654
PTPN11	ENST00000351677	2.36303	0.002438	1.851827	0.03007

Gene symbol	Ensembl ID	GSE86202		GSE151352	
		log2 (FC)	P-value	log2(FC)	P-value
RANBP6	ENST00000259569	-0.9764	0.010593	-0.9782	0.018178
RAPGEF5	ENST00000344041	-3.29659	0.011222	-3.87801	6.11E-09
RBM20	ENST00000369519	-1.49963	0.035341	-1.83547	0.000478
RERE	ENST00000337907	-0.71607	0.057925	-1.04612	0.046666
RP11-364B14.3	ENST00000453380	-3.07645	0.013006	-2.679	0.00647
RP11-548O1.3	ENST00000495287	-1.41003	0.005495	-1.19579	0.000307
RP11-573G6.6	ENST00000566763	-2.43661	3.79E-05	-2.98811	5.64E-05
SAMD4B	ENST00000314471	2.425298	0.032765	2.193776	0.009102
SH3BP2	ENST00000503393	2.999039	0.058144	2.351316	0.053821
SHMT1	ENST00000316694	1.376769	0.057446	0.478809	0.040998
SLC6A9	ENST00000372310	-2.9317	6.60E-06	-2.36244	0.003276
SMG6	ENST00000574501	-4.4652	0.001828	-1.94312	0.049293
SNORD116-6	ENST00000384711	-2.36355	0.000573	-3.4219	2.16E-07
SOX3	ENST00000370536	-2.86093	0.003264	-4.03012	5.4E-06
SPARC	ENST00000231061	1.541774	0.018242	0.809204	0.010656
SYNM	ENST00000561323	-1.16092	0.012187	-0.80428	0.047329
TEK	ENST00000380036	-1.08628	0.04334	-2.59451	0.016505
TNIK	ENST00000436636	-1.65314	0.022505	-3.661	0.001868
TNRC6C	ENST00000335749	0.711425	0.041801	0.628342	0.021548
TTN	ENST00000589042	-2.99415	0.000902	-2.42567	0.008926
U3	ENST00000391249	1.486661	0.011397	0.939354	0.001736
USP15	ENST00000280377	-1.76516	3.87E-05	-2.64442	0.033033
WASH7P	ENST00000423562	1.648156	0.022976	1.410344	0.022637
ZNF514	ENST00000496060	-0.74585	0.058723	-1.08466	0.03908
GLIS3	ENST00000324333	-2.7891	0.03567	2.77801	0.02682
FLRT2	ENST00000330753	-0.9836	0.011457	-1.322	0.054359
POLH	ENST00000372236	0.818777	0.0123	0.739577	0.053572
PPIL4	ENST00000253329	-1.1034	0.006928	-1.19579	0.000307

Furthermore, functional enrichment analysis of overlapped genes was identified (Fig. 4) and an interaction network was constructed, which included55 nodes and 189 edges (Fig. 5).

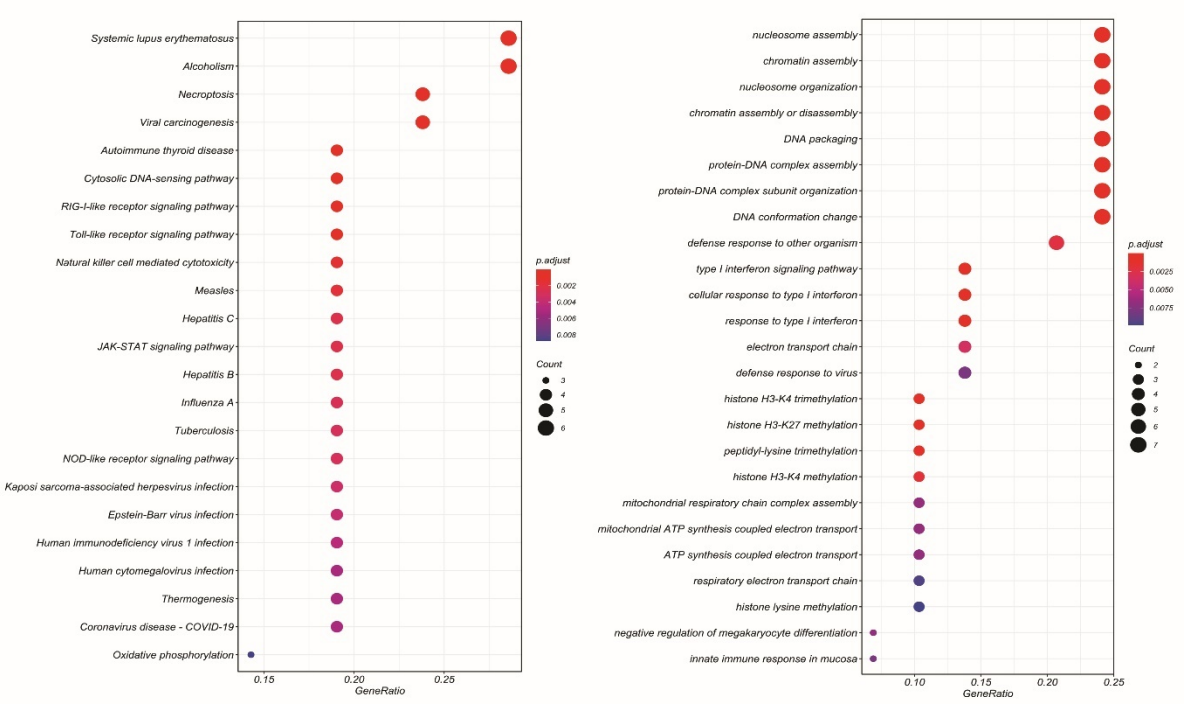

Fig. 4 Enrichment analysis of 109 overlapped genes. KEGG pathway (Left figure) and GO (Biological Process) function enrichment (Right figure).

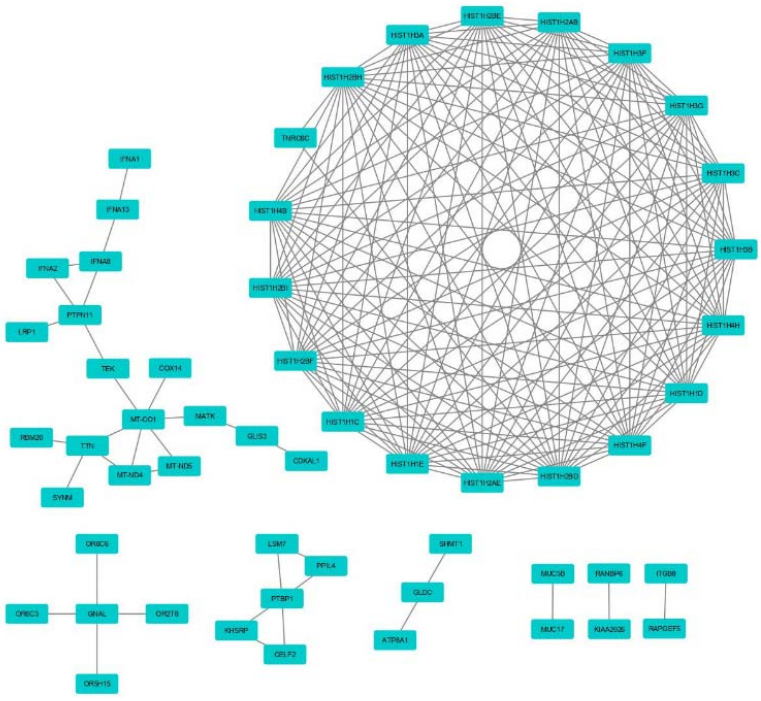

Fig. 5 Network of 109 overlapped genes. This network comprised of 55 nodes and 189 edges.

In addition, the cluster was investigated using the MCODE plugin including 25 nodes and 161 edges (Fig. 6).

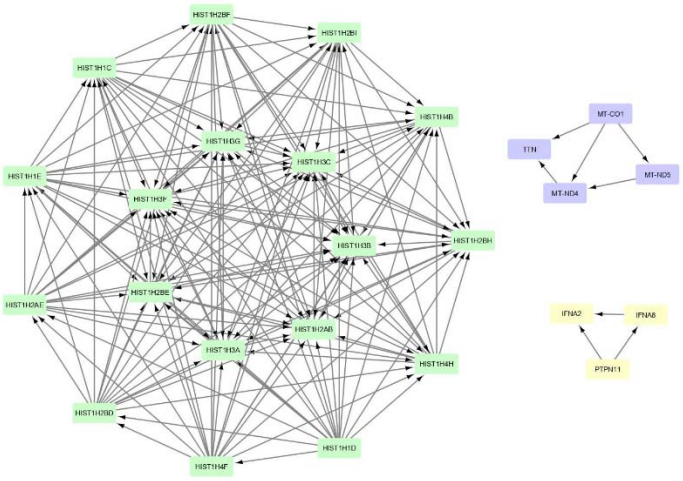

Fig. 6 Cluster analysis using the MCODE plugin. This network comprised of 25 nodes and 161 edges.

In the next step, the hub genes of the extracted clusters were examined based on 12 methods. (HIST1H2AE –HIST1H1C-HIST1H2AB) which are showed in Table 3 and the interaction network of hub genes was identified based on degree method that contains 18 nodes and 153 edges (Fig. 7).

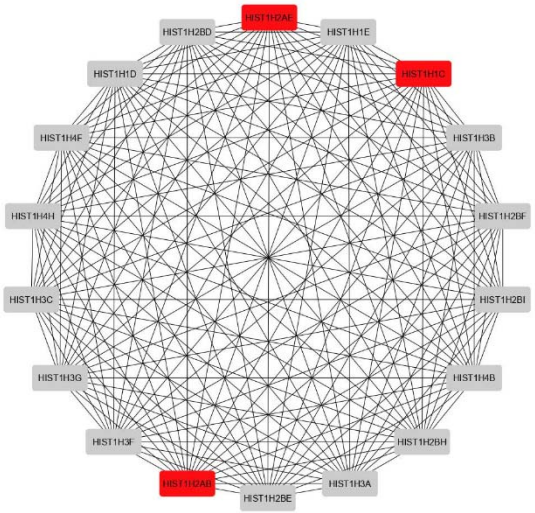

Fig. 7 Network of hub genes based on degree method. This network comprised of 18 nodes and 153 edges. In this network HIST1H2AE, HIST1H1C, and HIST1H2AB proteins had the most number of targets which are highlighted in red.

Table 3 Investigation of hub genes clusters based on 12 methods.

Node name	MCC	DMNC	MNC	Deg.	EPC	Bottle Neck	Ec Centricity	Closeness	Radiality	Betweenness	Stress	Clustering Coef.
IFNA8	2	0.30779	2	2	1.169	1	0.12	2	0.24	0	0	1
IFNA2	2	0.30779	2	2	1.18	1	0.12	2	0.24	0	0	1
PTPN11	2	0.30779	2	2	1.171	1	0.12	2	0.24	0	0	1
TTN	2	0.30779	2	2	1.226	1	0.08	2.5	0.42667	0	0	1
MT-ND5	2	0.30779	2	2	1.229	1	0.08	2.5	0.42667	0	0	1
MT-ND4	4	0.30898	3	3	1.313	1	0.16	3	0.48	1	2	0.66667
MT-CO1	4	0.30898	3	3	1.322	1	0.16	3	0.48	1	2	0.66667
HIST1H2BI	9.22E+13	1.10097	17	17	8.166	1	0.72	17	0.80471	0	0	1
HIST1H4B	9.22E+13	1.10097	17	17	8.394	1	0.72	17	0.80471	0	0	1
HIST1H2AB	9.22E+13	1.10097	17	17	8.059	1	0.72	17	0.80471	0	0	1
HIST1H2AE	9.22E+13	1.10097	17	17	8.186	1	0.72	17	0.80471	0	0	1
HIST1H3C	9.22E+13	1.10097	17	17	8.275	1	0.72	17	0.80471	0	0	1
HIST1H3B	9.22E+13	1.10097	17	17	8.316	1	0.72	17	0.80471	0	0	1
HIST1H3G	9.22E+13	1.10097	17	17	8.276	1	0.72	17	0.80471	0	0	1
HIST1H1C	9.22E+13	1.10097	17	17	8.163	1	0.72	17	0.80471	0	0	1
HIST1H3F	9.22E+13	1.10097	17	17	8.102	1	0.72	17	0.80471	0	0	1
HIST1H1E	9.22E+13	1.10097	17	17	8.205	1	0.72	17	0.80471	0	0	1
HIST1H3A	9.22E+13	1.10097	17	17	8.188	1	0.72	17	0.80471	0	0	1
HIST1H1D	9.22E+13	1.10097	17	17	8.145	1	0.72	17	0.80471	0	0	1
HIST1H2BD	9.22E+13	1.10097	17	17	8.273	1	0.72	17	0.80471	0	0	1
HIST1H4F	9.22E+13	1.10097	17	17	8.233	1	0.72	17	0.80471	0	0	1
HIST1H2BH	9.22E+13	1.10097	17	17	8.475	1	0.72	17	0.80471	0	0	1
HIST1H2BE	9.22E+13	1.10097	17	17	8.33	1	0.72	17	0.80471	0	0	1
HIST1H4H	9.22E+13	1.10097	17	17	8.529	1	0.72	17	0.80471	0	0	1
HIST1H2BF	9.22E+13	1.10097	17	17	8.283	1	0.72	17	0.80471	0	0	1

Among 109 common genes, 6 lncRNAs were obtained and the relationship between lncRNA and mRNA was examined using correlation testing based on expression data. These 6 lncRNAs had a correlation greater than 0.5 with 91 genes and negative correlations greater than -0.5 were not found. Using Cytoscape software, the interaction network was constructed only based on correlations greater than 0.5.Then CytoHubba plugin was used and lncRNAs associated with the largest number of genes that possessed the highest correlation were selected. Three lncRNAs were selected as hubs which correlated with 56 altered genes greater than 0.5 (Fig. 8).

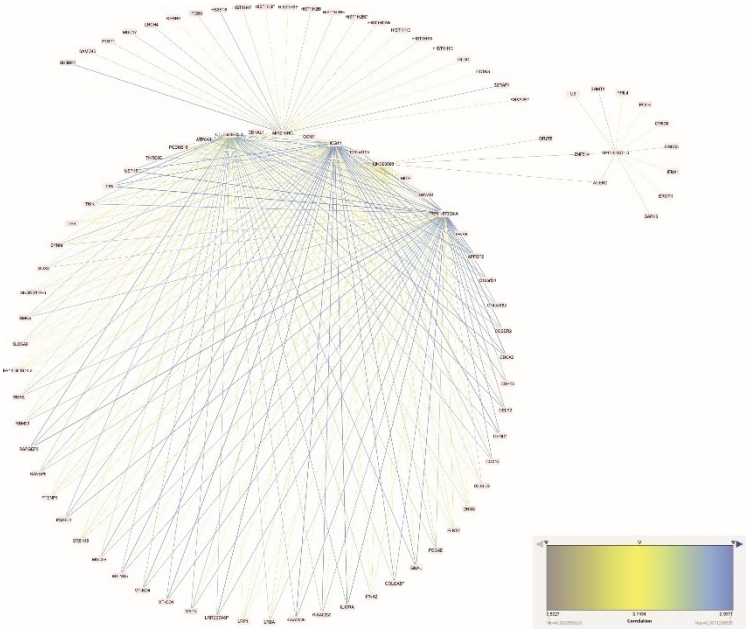

Fig. 8 Network related to the investigation of lncRNA correlation and DEGs. This network comprised of 93 nodes and 250 edges and the thickness and color of the edges are adjusted based on the correlation rate from 0.5 to 0.9 from thin to thick and according to the color scale in the image.

The network of hub lncRNAs was then identified. Hub lncRNA networks including 60 nodes and 213 edges were visualized, in which lncRNAs based on the degree of the largest number of targets, are marked in red, orange, and yellow (Fig. 9).

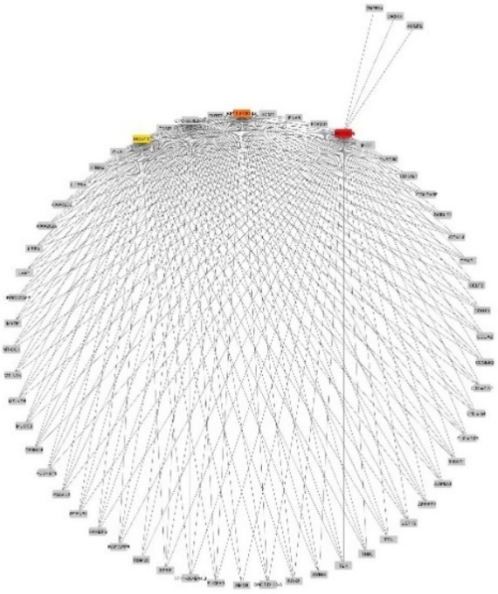

Fig. 9 Network of hub lncRNAs based on degree method. This network comprised of 60 nodes and 231 edges and lncRNAs which had the most of the targets are marked in red (LINC00598) – orange (RP11-573G6.6) and yellow (HCG11) respectively.

LINC00598, RP11-573G6.6, and HCG11 were selected as significant lncRNAs, respectively, all three of which have showed decreased expression in GBM compared to the controls and have been selected as hubs in this study. In addition, these three lncRNAs are also related to IFNA2, IFNA8, MT-CO1, MT-ND4, MT-ND5, and TTN which are obtained from MCODE clusters. The highest associations are between RP11-573G6.6, and HCG11 with MT-CO1, MT-ND4, MT-ND5, and TTN. Decreased expression of HCG11 in GBM has previously been reported. In this study decreased expression of lncRNA RP11-573G6.6 is reported as a novel result, which is associated with decreased expression of mitochondrial genes. Moreover, the network between lncRNA and the MCODE cluster genes were constructed in which the correlation number on the edge is specified (Fig. 10).

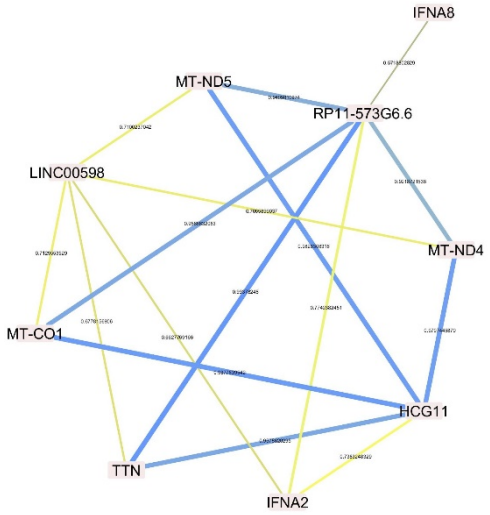

Fig. 10 The network between lncRNA and MCODE cluster genes. The thickness and color of the edges in this network are adjusted based on the correlation rate from the highest ratio (the thickest edge in blue) to the lowest one (thin and yellow in color). The correlation scores are shown on the edges.

4 Discussion

In recent years, with technological advances in high-throughput screening, lncRNAs are rapidly being identified and characterized (Yang et al., 2014). Based on growing evidence, lncRNAs play an important role in fundamental biological processes and also attracted much attention. Therefore, it is not surprising that lncRNAs have been implicated in various human diseases, including the development and progression of various cancers (Wilusz et al., 2009; Managadze et al., 2011). In particular, although many experimental studies have been performed on lncRNAs, only a few of them have been extensively investigated that have identified potential links to different cancers, including GBM. Predicting the association between lncRNA and various diseases in different fields of biology and medicine is of great importance. Recently, scientists have focused on *in silico* studies for predicting new disease-related lncRNAs, which help to understand the biogenesis, regulation, and function of lncRNAs, and the molecular mechanism of human disease (Taft et al., 2010; Chen et al., 2015; Chen and Yan 2013; Chen 2015a, 2015b). Based on computational models, disease-related lncRNAs with higher scores can be selected for further experimental validation. In other words, bioinformatics methods can provide powerful guidance for research to identify new lncRNA related to human diseases. Computational approaches can also be used to predict the potential functions of lncRNAs, identify new lncRNAs, and build regulatory networks (Mohanty et al., 2015). Network analysis can be considered as a powerful and efficient tool in predicting the potential association of lncRNA with human diseases and can

have a profound impact on the prognosis, diagnosis, and treatment of diseases at the lncRNA level (Chen et al. 2017). In this paper, we summarized the functions of lncRNAs, introduced important lncRNAs related to GBM, some important pathways, and biological processes, etc. This disease has a poor prognosis and remains an incurable disease. With recent advances, molecular mechanisms have provided opportunities for the development of effective treatments for this tumor. We found two lncRNAs that could be used as the promising and novel GBM-related lncRNAs for biological experiment validation. RNA-seq data was used to find lncRNAs related to GBM. Some approaches also were used to search for pathways and biological processes that are implicated in a process of GBM. Totally, based on the P-value score and network analysis, the potential role of LINC00598, RP11-573G6.6, and HCG11 as significant lncRNAs in GBM was elucidated. LINC00598 (LncFOXO1) suppresses the growth of breast cancer (BC) cells in humans through BAP1. In fact, lncFOXO1 is involved in suppressing BC growth by increasing FOXO1 transcription. Besides, lncFOXO1 is associated with BRCA-1-associated protein 1 (BAP1) and controls its binding and also the level of mono-ubiquitinated H2A at K119 (ubH2AK119) at FOXO1 promoter. lncFOXO1 is considerably reduced in both BC tissues and cell lines, and there is a correlation between the down regulation of lncFOXO1 and poorer overall survival (Xi et al., 2017). Also, HCG11 was down regulated in both glioma tissues and cell lines. Besides, low HCG11 levels show a decline in the overall survival rate of GBM patients. HCG11 was also present in the cytoplasm of glioma cells and released MTA3 expression by interacting with miR-4425 (Zhang et al., 2019). HCG11 expression levels are lower in glioma samples compared to normal subjects.FOXP1 can bind to HCG11 and inactivate it at the transcriptional level. Overexpression of HCG11 efficiently leads to cell proliferation, cell cycle arrest, and increased cell apoptosis. HCG11 is enriched in the cytoplasm of glioma cells and represented a competing endogenous RNAs (ceRNAs) role using sponging micro-496 to upregulate cytoplasmic polyadenylation element binding protein 3 (CPEB3).CEPB3 and miR-496 are implicated in HCG11-mediated glioma development (Chen et al., 2019). In addition, HCG11 acts as a tumor suppressor in prostate cancer and is also dysregulated in BC as well as gastric cancer (Liu et al., 2016; Zhang et al., 2016). Moreover, the TTN protein is encoded by *Ttn* and is responsible for the passive elasticity of cells. A mutation leading to an altered TTN was associated with GBM (Balakrishnan et al., 2007).

5 Conclusion

In conclusion, we have identified the role of RP11-573G6.6 and HCG11 based on *in silico* analysis in GBM. The present study has also shown the cellular and biological role of both lncRNAs and identified potential molecular interaction partners and furthermore suggested that they play key roles in GBM pathogenesis and can be exploited as promising targets in effective management, and novel therapeutic approaches.

Acknowledgements

We would like to thanks to DNA Raya Zist Company, Isfahan, Iran.

References

Afgan E, Baker D, Batut B, Van Den Beek M, Bouvier D, Čech M, Chilton J, et al. 2018. The Galaxy platform for accessible, reproducible and collaborative biomedical analyses: 2018 update. Nucleic Acids Research, 46: W537-W544

Alifieris C, Trafalis DT. 2015. Glioblastoma multiforme: Pathogenesis and treatment. Pharmacology and Therapeutics, 152: 63-82

Andrews S. 2010. FastQC: A Quality Control Tool For High Throughput Sequence Data. Babraham Bioinformatics, Babraham Institute, Cambridge, United Kingdom

Bai RY, Staedtke V, Riggins GJ. 2011. Molecular targeting of glioblastoma: drug discovery and therapies. Trends in Molecular Medicine, 17: 301-312

Balakrishnan A, Bleeker FE, Lamba S, Rodolfo M, Daniotti M, Scarpa A, et al. 2007. Novel somatic and germline mutations in cancer candidate genes in glioblastoma, melanoma, and pancreatic carcinoma. Cancer Research, 67: 3545-3550.

Chen X. 2015a. KATZLDA: KATZ measure for the lncRNA-disease association prediction. Scientific reports, 5**,** 1-11.

Chen X. 2015b. Predicting lncRNA-disease associations and constructing lncRNA functional similarity network based on the information of miRNA. Scientific Reports, 5: 1-11

Chen X, Yan CC, Luo C, Ji W, Zhang Y, Dai Q. 2015. Constructing lncRNA functional similarity network based on lncRNA-disease associations and disease semantic similarity. Scientific Reports, 5: 1-12

Chen X, Yan CC, Zhang X, You ZH. 2017. Long non-coding RNAs and complex diseases: from experimental results to computational models. Briefings in Bioinformatics, 18: 558-576

Chen X, Yan GY. 2013. Novel human lncRNA–disease association inference based on lncRNA expression profiles. Bioinformatics, 29: 2617-2624

Chen Y, Bao C, Zhang X, Lin X, Huang H, Wang Z. 2019. Long non-coding RNA HCG11 modulates glioma progression through cooperating with miR-496/CPEB3 axis. Cell Proliferation, 52: e12615

Chin CH, Chen SH, Wu HH, Ho CW, Ko MT, Lin CY. 2014. cytoHubba: identifying hub objects and sub-networks from complex interactome. BMC Systems Biology, 8: 1-7

Ducray F, Hallani S El, Idbaih A. 2009. Diagnostic and prognostic markers in gliomas. Current Opinion in Oncology, 21: 537-542

Fang Y, Fullwood MJ. 2016. Roles, functions, and mechanisms of long non-coding RNAs in cancer. Genomics, Proteomics and Bioinformatics, 14: 42-54

Huarte M. 2015. The emerging role of lncRNAs in cancer. Nature Medicine, 21: 1253-1261

Kim D, Paggi JM, Park C, Bennett C, Salzberg SL. 2019. Graph-based genome alignment and genotyping with HISAT2 and HISAT-genotype. Nature Biotechnology, 37: 907-915

Liu H, Li J, Koirala P, Ding X, Chen B, Wang Y, Wang Z, Wang C, Zhang X, Mo XY. 2016. Long non-coding RNAs as prognostic markers in human breast cancer. Oncotarget, 7: 20584

Louis DN, Perry A, Reifenberger G, Von Deimling A, Figarella-Branger D, Cavenee WK, et al. 2016. The 2016 World Health Organization classification of tumors of the central nervous system: a summary. Acta Neuropathologica, 131: 803-820

Love M, Anders S, Huber W. 2014. Differential analysis of count data–the DESeq2 package. Genome Biology, 15: 10.1186

Managadze D, Rogozin IB, Chernikova D, Shabalina SA, Koonin EV. 2011. Negative correlation between expression level and evolutionary rate of long intergenic noncoding RNAs. Genome Biology And Evolution, 3: 1390-1404

Mohanty V, Goekmen-Polar Y, Badve S, Janga SC. 2015. Role of lncRNAs in health and disease—size and shape matter. Briefings in functional genomics, 14: 115-129

Parker NR, Khong P, Parkinson JF, Howell VM, Wheeler HR. 2015. Molecular heterogeneity in glioblastoma: potential clinical implications. Frontiers in Oncology, 5: 55

Pertea M, Pertea GM, Antonescu CM, Chang TC, Mendell JT, Salzberg SL. 2015. StringTie enables improved reconstruction of a transcriptome from RNA-seq reads. Nature Biotechnology, 33: 290-295

Ponting CP, Oliver PL, Reik W. 2009. Evolution and functions of long noncoding RNAs. Cell, 136: 629-641

Qureshi IA, Mehler MF. 2012. Emerging roles of non-coding RNAs in brain evolution, development, plasticity and disease. Nature Reviews Neuroscience, 13: 528-541

Sánchez Y, Huarte M. 2013. Long non-coding RNAs: challenges for diagnosis and therapies. Nucleic Acid Therapeutics, 23: 15-20

Shannon P, Markiel A, Ozier O, Baliga NS, Wang JT, Ramage D, Amin N, Schwikowski B, Ideker T. 2003. Cytoscape: a software environment for integrated models of biomolecular interaction networks. Genome Research, 13: 2498-2504

Szklarczyk D, Franceschini A, Wyder S, Forslund K, Heller D, Huerta-Cepas J, Simonovic M, et al. 2015. STRING v10: protein–protein interaction networks, integrated over the tree of life. Nucleic Acids Research, 43: D447-D452

Taft RJ, Pang KC, Mercer TR, Dinger M, Mattick JS. 2010. Non-coding RNAs: regulators of disease. The Journal of Pathology: A Journal of the Pathological Society of Great Britain and Ireland, 220: 126-139

Van Meir EG, Hadjipanayis CG, Norden AD, Shu HK, Wen PY, Olson JJ. 2010. Exciting new advances in neuro-oncology: the avenue to a cure for malignant glioma. CA: A Cancer Journal For Clinicians, 60: 166-193

Wilusz JE, Sunwoo H, Spector DL. 2009. Long noncoding RNAs: functional surprises from the RNA world. Genes and Development, 23: 1494-1504

Xi J, Feng J, Li Q, Li X, Zeng S. 2017. The long non-coding RNA lncFOXO1 suppresses growth of human breast cancer cells through association with BAP1. International Journal of Oncology, 50: 1663-1670

Yang G, Lu X, Yuan L. 2014. LncRNA: a link between RNA and cancer. Biochimica et Biophysica Acta - Gene Regulatory Mechanisms, 1839: 1097-1109

Yoon JH, Abdelmohsen K, Srikantan S, Yang X, Martindale JL, De S, Huarte M, Zhan M, et al. 2012. LincRNA-p21 suppresses target mRNA translation. Molecular Cell, 47: 648-655

Zhang L, Cao Y, Kou X, Che L, Zhou X, Chen G, Zhao J. 2019. Long non-coding RNA HCG11 suppresses the growth of glioma by cooperating with the miR-4425/MTA3 axis. The Journal of Gene Medicine, 21: e3074

Zhang Y, Zhang P, Wan X, Su X, Kong Z, Zhai Q, Xiang X, Li L, Li Y. 2016. Downregulation of long non-coding RNA HCG11 predicts a poor prognosis in prostate cancer. Biomedicine and Pharmacotherapy, 83: 936-941

Zhou Y, Dai W, Wang H, Pan H, Wang Q. 2018. Long non-coding RNA CASP5 promotes the malignant phenotypes of human glioblastoma multiforme. Biochemical and Biophysical Research Communications, 500: 966-972